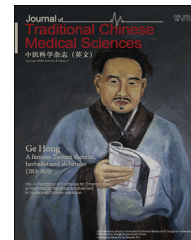ELSEVIER

Since January 2020 Elsevier has created a COVID-19 resource centre with free information in English and Mandarin on the novel coronavirus COVID-19. The COVID-19 resource centre is hosted on Elsevier Connect, the company's public news and information website.

Xijiao Dihuang Decoction combined with Yinqiao Powder reverses influenza virus-induced F-actin reorganization in PMVECs by inhibiting ERM phosphorylation

Zinan Xuan [a], Ying Wu [a,*], Chenyue Zhang [b], Shujing Zhang [a],
Xiangyang Chen [a], Shuyu Li [a], Yu Hao [a], Qian Wang [a],
Xudan Wang [a], Shu Zhang [a]

[a] Department of Microbiology and Immunology, Beijing University of Chinese Medicine, Beijing 100029, PR China
[b] Department of Integrative Oncology, Fudan University Shanghai Cancer Center, Shanghai 200032, PR China

Abstract *Objective:* It has been documented that ezrin/radixin/moesin (ERM) phosphorylation by the p38 mitogen-activated protein kinase (MAPK), Rho/ROCK, and protein kinase C (PKC) pathways leads to filamentous actin (F-actin) reorganization and microvascular endothelial cell hyperpermeability. In this study, we investigated the effects of Xijiao Dihuang Decoction combined with Yinqiao Powder (XDY) on influenza virus (IV)-induced F-actin restructuring and ERM phosphorylation regulated by the Rho/Rho kinase 1 (ROCK), p38 MAPK, and PKC signaling pathways in pulmonary microvascular endothelial cells (PMVECs).

Methods: Serum containing XDY (XDY-CS; 13.8 g/kg) was acquired using standard protocols for serum pharmacology. Primary PMVECs were obtained from male Wistar rats and cultured. After adsorption of IV A (multiplicity of infection, 0.01) for 1 h, medium with 20% XDY-CS was added to the PMVECs. The distributions of F-actin and phosphorylated ERM were determined by confocal microscopy, and F-actin expression was measured by flow cytometry. The expression levels of ROCK1, phosphorylated myosin phosphatase target-subunit (p-MYPT), phosphorylated MAPK kinase, phosphorylated p38 (p-p38), phosphorylated PKC (p-PKC), and phosphorylated ERM (p-ERM) were determined by western blotting.

Results: F-actin reorganization in IV-infected PMVECs was reversed by XDY-CS treatment, which was accompanied by reduced p-ERM production. The p-ERM protein accumulated at plasma membrane of PMVECs infected with IV, which was also inhibited by XDY-CS treatment.

* Corresponding author. Tel.: +86 10 64286973; fax: +86 10 64286871.
E-mail address: aqiwuying@hotmail.com (Y. Wu).
Peer review under responsibility of Beijing University of Chinese Medicine.

In addition, XDY-CS treatment drastically reduced the levels of p-p38, ROCK1, p-MYPT, and p-PKC induced by IV infection in PMVECs.

Conclusion: These results show that XDY-CS inhibited influenza-induced F-actin reorganization in PMVECs by down-regulating p-ERM expression via inhibition of the Rho/ROCK, p38 MAPK, and PKC pathways. In conclusion, XDY could reduce the damage to endothelial cytoskeleton induced by IV infection, thus protecting the barriers of PMVECs.

Introduction

Influenza virus (IV) is a prevalent virus that causes respiratory diseases worldwide. Seasonal viruses spreading among the human population cause annual epidemics that lead to approximately 500 000 deaths per year. One of the major health complications of IV is viral pneumonia, which can result in acute respiratory distress syndrome (ARDS).[1] In the acute phase of ARDS, symptoms are characterized by cyanosis, hypoxemia, pulmonary edema, and respiratory failure, which may ultimately lead to multiple organ failure and a low survival rate.[2]

Respiratory failure in the acute phase of ARDS can be attributed to damage to the epithelial-endothelial barriers of pulmonary alveoli, where gas exchange takes place.[3,4] Damage to these barriers leads to the flooding of proteinaceous edema fluid containing fibrin, erythrocytes, and inflammatory cells into the alveolar lumen. Although the pathogenesis of ARDS is only partially understood, it is thought that the key determinants of ARDS are endothelial barrier dysfunction and subsequent pulmonary microvascular endothelial leakage. Clinical analysis showed that mortality remains high among patients with severe influenza despite the use of anti-viral therapeutic strategies, which suggests that microvascular leakage may play a critical role in the pathogenesis of viral infections.[5]

Xijiao Dihuang Decoction combined with *Yinqiao* Powder (XDY) is a classic compound formula originally prescribed by Jutong Wu, an ancient Chinese physician from the Qing Dynasty. XDY can clear heat, remove toxins, cool blood, stop bleeding, and promote blood circulation.[6] Results from a clinical study indicated that modified *Yinqiao* Powder could ameliorate symptoms and shorten the duration of fever caused by H1N1 IV.[7] *Xijiao Dihuang* Decoction, currently referred to as *Qingre Dihuang* Decoction, has been evaluated as a treatment for blood-heat syndrome in modern studies. *Xijiao Dihuang* Decoction was beneficial in treating syndromes where toxins intrude into the blood, a phenomenon that occurs in severe acute respiratory syndrome (SARS).[8] For example, modified *Xijiao Dihuang* Decoction was used to treat fire-toxin syndrome caused by viral pneumonia by virtue of its abilities for clearing heat, cooling blood, nourishing yin, and dispelling phlegm.[9] In previous studies, we showed that XDY treatment clearly reduced the mortality rate, decreased pulmonary permeability, and alleviated pulmonary edema in mice with viral pneumonia.[10] The results from in vitro studies demonstrated that XDY could protect the endothelial barrier by reversing permeability increases in PMVECs caused by IV infection.[11] However, the mechanisms by which XDY mitigates hyper-permeability in IV-infected PMVECs requires further investigation.

The Ezrin/Radixin/Moesin (ERM) protein forms links between the cytomembrane and the cytoskeleton. The integrity of the cytoskeleton is mediated by ERM phosphorylation and is crucial for the maintenance of both endothelial morphology and permeability. It has been well documented that ERM can be phosphorylated via the p38 mitogen-activated protein kinase (MAPK), Rho/Rho kinase (ROCK), and protein kinase C (PKC) pathways, thus leading to rearrangement of filamentous actin (F-actin) and hyper-permeability of microvascular endothelial cells.[12–14]

Therefore, in this study, we focused on the effects of XDY on F-actin rearrangement in IV-infected PMVECs. Furthermore, we explored the underlying mechanisms by determining its effects on ERM phosphorylation, as well as its roles in activating the Rho/ROCK, p38 MAPK, and PKC pathways, which serve as upstream activators of the ERM protein.

Materials and methods

Reagents

Dulbecco's modified Eagle's medium, Medium 199 (M199), and fetal bovine serum (FBS) were purchased from Thermo Fisher Scientific (Waltham, MA, USA). Endothelial cell growth supplement (ECGS) was purchased from Becton, Dickinson and Company (Bergen, NJ, USA). Fluorescein isothiocyanate labeled-phalloidin (phalloidin-FITC) was purchased from Sigma–Aldrich (St Louis, MO, USA). The reagent 4′,6-diamidino-2-phenylindole (DAPI) was purchased from Boster (Wuhan, Hubei, China). Bovine serum albumin (BSA) was obtained from Amresco (Solon, OH, USA). Paraformaldehyde and Triton-X-100 were purchased from Beijing Bioway Biotech Group (Beijing, China). Antibodies against phosphorylated ERM (p-ERM) and phosphorylated PKC (p-PKC) were obtained from Cell Signaling Technology (Danvers, MA, USA). Antibodies against phosphorylated MAPK kinase (p-MKK), phosphorylated p38 (p-p38), and ROCK1 were purchased from Abcam (Cambridge, England, UK). An antibody against phosphorylated myosin phosphatase target-subunit (p-MYPT) was purchased from Abnova (Taipei, Taiwan, China). Recombinant

glyceraldehyde-3-phosphate dehydrogenase (GAPDH) was obtained from Proteintech (Chicago, IL, USA). A DyLight594-conjugated goat anti-rabbit secondary antibody was purchased from Beijing ComWin Biotech (Beijing, China). β-actin was obtained from Santa Cruz Biotechnology (Dallas, Texas, USA). The Enhanced Chemiluminescence (ECL) Western Blot Detection System and polyvinylidene fluoride (PVDF) membranes were obtained from Millipore (Bedford, MA, USA). Madin—Darby canine kidney (MDCK) cells were obtained from the Chinese Academy of Medical Sciences (Shanghai, China).

Preparation of XDY

Thirty grams of rhinoceros horn (*Rhinoceros nicornis LR.simus Burchell*) (replaced with bubali cornu now), 30 g of rehmanniae radix (*Rehmannia glutinosa (Gaetn.) Libosch.*), 12 g of paeoniae radix rubra (*Paeonia lactiflora Pall.*), 9 g of moutan cortex (*Paeonia suffruticosa Andr.*), 9 g of forsythiae fructus (*Forsythia suspensa (Thunb.) Vahl*), 9 g of lonicerae japonicae flos (*Lonicera japonica Thunb.*), 6 g of platycodonis radix (*Platycodon grandiflorum (Jacq.) A.DC.*), 6 g of menthae herba (*Mentha haplocalyx Briq.*), 4 g of lophatheri herba (*Lophatherum gracile Brongn.*), 5 g of glycyrrhizae radix (*Glycyrrhiza uralensis Fisch.*), 5 g of schizonepetae herba (*Schizonepeta tenuifolia Briq.*), 5 g of sojae semen praeparatum (*Glycine max (L.) Merr.*), and 9 g of arctii fructus (*Arctium lappa L.*) were purchased from Dongzhimen Hospital, Beijing University of Chinese Medicine. These materials were soaked in distilled water for 1 hour then boiled the first time in water (w/v, 1/10) for 1 hour and 15 min, and then boiled the second time in water (w/v, 1/6) for 15 minutes. The resulting solution was concentrated to a final density of 2.07 g/mL.

Preparation of XDY-containing serum (XDY-CS)

The study was performed according the "Principles of Laboratory Animal Care" guidelines published by the World Health Organization.[15] And experiments were approved by the Institutional Animal Ethics Committee of Beijing University of Chinese Medicine. Male Wistar rats weighing 270—310 g were obtained from Vital River Laboratories (Beijing, China) and randomly divided into 2 groups: (1) XDY-CS group: 10 rats were administered XDY solution by intragastric gavage in twice-daily doses of 13.8 g/kg (4 mL/rat) for 3 days. This dose was equal to 6 times that used previously with adult-dosage. (2) Control serum (Con-S) group: 10 rats were administered saline using the same treatment schedule and volumes described for the XDY-CS group. At 1 hour after the last administration, blood was obtained from abdominal the aorta and stored at $25 \pm 1°C$ for 4 h. Serum was isolated by centrifugation (3000 rpm, 15 minutes), inactivated at 56°C for 30 min, and stored at $-70°C$ in preparation for further experiments.

IV propagation

Mouse-adapted IV strain A/FM/1/47 was purchased from the Institute of Virus Research in the Chinese Center for Disease Control and Prevention, and was propagated in 9-day-old embryonated eggs (Beijing Merial Vital Laboratory Animal Technology (Beijing, China).). The 50% tissue culture-infectious dose ($TCID_{50}$) was determined by performing a cytopathic effect (CPE) assay, according to the method of Reed and Muench. The $TCID_{50}$ of IV strain A/FM/1/47 was $10^{-4.6}$/mL. PMVECs were infected with IV at a multiplicity of infection (MOI) of 0.01.

Rat PMVEC culture

Four-week-old, male Wistar rats weighing 70—90 g were obtained from Vital River Laboratories (Beijing, China). PMVECs were isolated and cultured according to previous methods,[16,17] with some modifications. Briefly, 1-mm-thick tissue samples were removed from periphery of fresh lungs separated from rats and cut into 1-mm^3 pieces. Next, 25 of the 1-mm^3 lung pieces were placed in 1% gelatin-coated T25 cell flasks. The flasks were inverted and placed in an incubator (37°C, 5% CO_2) for 2 h, after which the flasks were stood upright and 1 mL of medium was added to each flask. The medium comprised M199 supplemented with 20% FBS, ECGS (100 μg/mL), and 1% penicillin-streptomycin solution. After a 60-h incubation, the tissues were abandoned, and 5 mL medium was added to individual T25 flasks. At approximately 90% confluence, the PMVECs were detached using 0.25% trypsin/0.02% EDTA and subcultured into new T25 flasks. PMVECs were identified according to morphological and functional criteria, and confluent PMVECs from the first 3 passages were used for experiments conducted with 3 groups. Cells in the control group were incubated with M199 containing 20% Con-S. Cells in the virus group were infected with IV A (MOI, 0.01) for 1 hour, and then incubated with M199 containing 20% Con-S. Cells in the XDY group were infected with IV A (MOI, 0.01) for 1 hour, and then incubated with M199 containing 20% XDY-CS. After the cells in each group were incubated for 24 h, they were used for the experiments described in Sections 2.6—2.8.

Flow cytometry

After washing PMVECs growing in 6-well plates twice with phosphate buffered saline (PBS), they were collected and fixed in 4% paraformaldehyde at 4°C. After permeabilization with 0.25% Triton-100, the cells were labeled for 40 minutes with 1 μg/mL phalloidin-FITC. Samples were then evaluated using a FACSCanto flow cytometer (Becton Dickinson, San Jose, CA), and the data were analyzed using BD FACS Diva software.

Confocal microscopy

PMVECs grown in 8-well RS glass side (Nunc, Denmark) were washed with PBS, fixed using 4% paraformaldehyde at 4°C, permeabilized using 0.5% Triton X-100, and blocked using 5% BSA. PMVECs were then incubated with an anti-p-ERM

antibody (1:400), followed by a DyLight 649-conjugated secondary antibody (1:800). F-actin was labeled using phalloidin-FITC (1 μg/mL) after the cells were pre-incubated with BSA. The images were collected with an FV1000 confocal microscope (Olympus, Japan).

Western blotting

After XDY-CS administration, cells were collected with a cell scraper and lysed in RIPA buffer. The lysate was centrifuged at 4°C (12,000 rpm, 30 min), and the total amount of protein contained in the supernatant was detected by using a BCA kit (Applygen, Beijing, China). Equivalent total protein samples were separated by 5% sodium dodecyl sulfate polyacrylamide gel electrophoresis and electro-transferred onto a PVDF membrane. The membranes were blocked with 5% nonfat milk for 1 hour at 27°C and then incubated with a corresponding primary antibody at 4°C overnight. After incubation with a secondary antibody at 27°C for 1 hour on the following day, immune-reactive bands were detected using the ECL Plus Western Blotting Detection Kit (Wuhan Boster Biotech Group, Hubei, China). The levels of p-ERM, p-p38, p-MKK, ROCK1, p-MYPT, and p-PKC were examined using corresponding primary antibodies diluted 1:1000, 1:2000,

1:800, 1:3000, 1:20, and 1:1000 in 5% nonfat milk, respectively.

Statistical analysis

Results are reported as the mean (SEM). Data were analyzed by student's t test for data between 2 groups using Prism software, version 5.0c (GraphPad Software, USA). The differences were considered significant when $P < .05$.

Results

Effect of XDY-CS on IV-induced F-actin reorganization

PMVECs in the control group showed a normal, spindle-shaped morphology. In the control group, a continuous F-actin distribution was observed mainly in the cortical areas of cells without stress fibers. In the virus group, F-actin in PMVECs reorganized, showing thickening and bundling in the cytoplasm, with the formation of thick stress fibers. Growth in the presence of XDY-CS reversed the F-actin rearrangement observed in IV-infected PMVECs. Cytoplasmic F-actin accumulation and stress fiber formation induced by IV infection were also alleviated by XDY-CS treatment (Fig. 1).
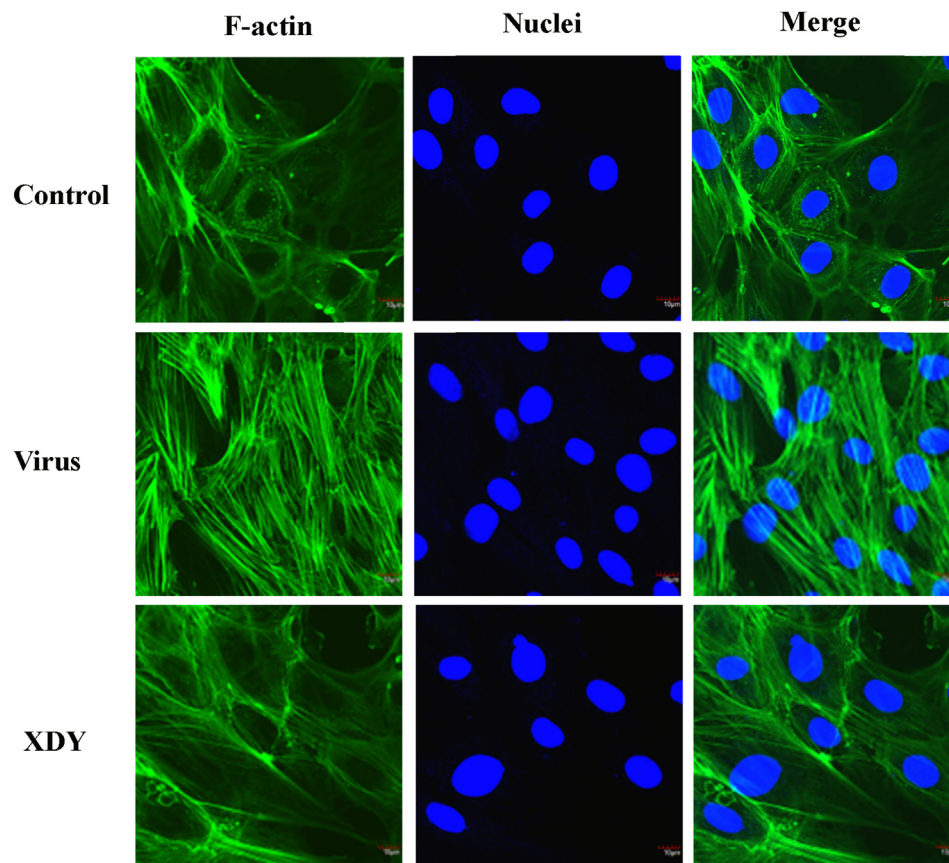

Fig. 1   Effect of XDY-CS on IV-induced F-actin reorganization (×60). Scale bars: 10 μm. After PMVECs were infected with IV and grown in medium containing XDY-CS for 24 h, F-actin in the cytoskeleton (green) and nuclei (blue) were examined using confocal microscopy. Three independent experiments were performed in triplicate.

Effect of XDY-CS on IV-induced F-actin up-regulation

In the virus group, F-actin expression in PMVECs increased remarkably, compared with that observed in the normal group ($P < .05$). IV-dependent F-actin induction was reduced in the XDY group; however, the difference between the virus group and the XDY group was not significant ($P > .05$; Fig. 2).

Effect of XDY-CS on the p-ERM level in IV-infected PMVECs

In the virus group, the p-ERM level significantly increased, compared with that observed in the control group ($P < .01$). The difference in p-ERM levels between the virus and XDY-CS groups was statistically significant, which implied that XDY-CS inhibited IV-induced ERM phosphorylation in PMVECs ($P < .05$; Fig. 3).

Effect of XDY-CS on p-ERM distribution in IV-infected PMVECs

Weak fluorescent detection of p-ERM in PMVECs was observed with the control group. p-ERM relocated to the border and showed enhanced detection in IV-infected PMVECs, as compared with that observed with the control group. XDY-CS treatment inhibited IV-induced p-ERM expression and redistribution to the periphery of PMVECs (Fig. 4).

Effect of XDY-CS on p-MKK and p-p38 production in IV-infected PMVECs

IV infection promoted significantly higher p-p38 and p-MKK production in PMVECs ($P < .001$), compared with that observed in the control group (Fig. 5). The p-p38 level was approximately 3-fold higher in the virus group relative to the control group, and p-MKK production was
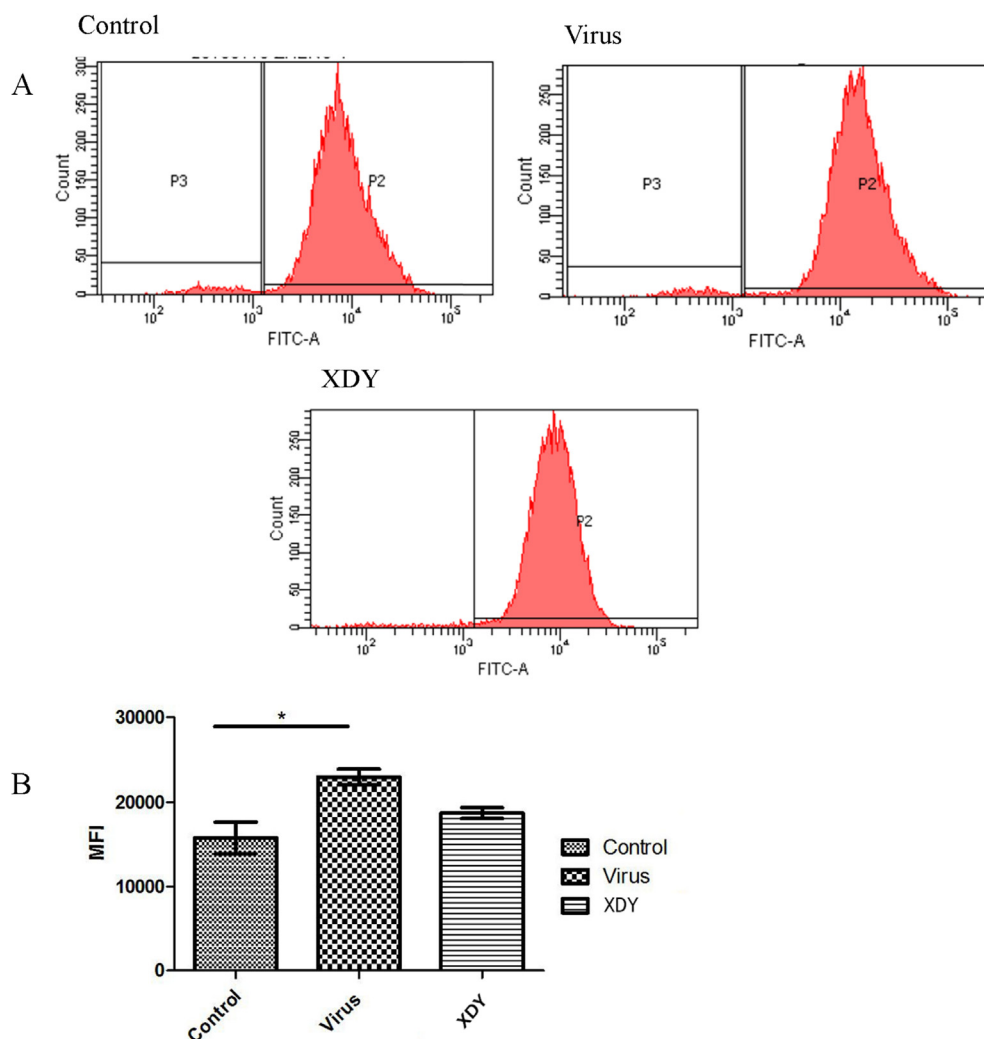

Fig. 2 Effect of XDY-CS on IV-induced F-actin up-regulation. (A) Effect of XDY-CS on virus-induced F-actin up-regulation, as determined by flow cytometry. (B) MFI levels. After PMVECS were treated as indicated for 24 h, F-actin expression was measured by flow cytometry. F-actin MFIs were calculated using Image software. Three independent experiments were performed in triplicate. Data are expressed as the mean (SEM). *: $P < .05$.
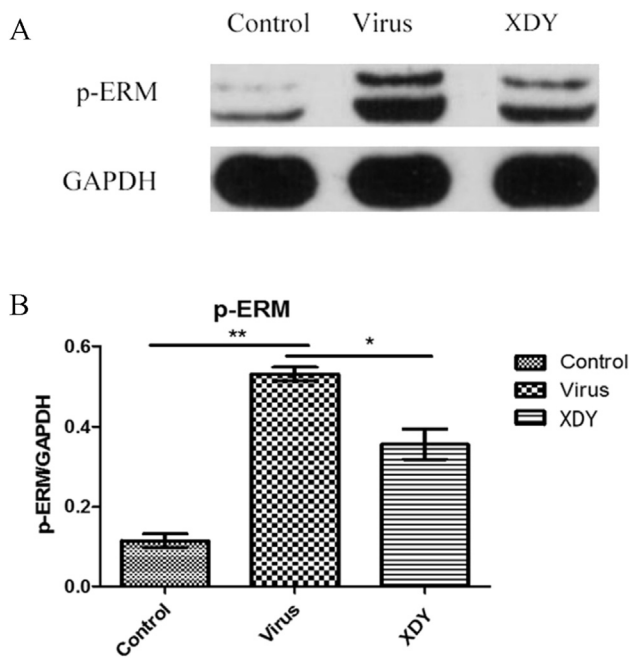
Fig. 3 Effect of XDY-CS on p-ERM production in IV-infected PMVECs. (A) Western blot analysis of p-ERM production in PMVECs. GADPH was detected as an internal reference. (B) Quantitative evaluation of p-ERM bands by densitometry. PMVECs were harvested 24 h after the indicated treatments and analyzed by western blotting using an anti-p-ERM antibody. Three independent experiments were performed in triplicate. Data are expressed as the mean (SEM). *: $P < .05$; **: $P < .01$.

approximately 2-fold higher. Treatment with XDY significantly attenuated IV-induced p38 phosphorylation ($P < .05$). Although p-MKK production in the XDY group was lower than that in the virus group, the difference was not statistically significant ($P > .05$). These data suggested that XDY might inhibit IV-induced activation of the p38 MAPK pathway.

Effect of XDY-CS on ROCK1 and p-MYPT levels in IV-infected PMVECs

To determine whether ERM is phosphorylated by the Rho/ROCK pathway and whether such phosphorylation can be inhibited by XDY-CS, we first assessed ROCK1 expression by western blotting. The production of p-MYPT was also studied because MYPT is a main substrate of ROCK that regulates myosin light chain phosphatase (MLC) phosphorylation. IV infection significantly increased ROCK1 and p-MYPT levels ($P < .001$) compared with those in the control group. Treatment with XDY-CS significantly downregulated virus-induced ROCK1 and p-MYPT overexpression in PMVECs ($P < .001$, $P < .001$; Fig. 6).

Effect of XDY-CS on p-PKC production in IV-infected PMVECs

The production of p-PKC was significantly increased by IV infection ($P < .05$), compared with that in the control

group. As expected, XDY-CS treatment significantly reduced p-PKC levels in IV-infected PMVECs ($P < .05$). These data indicated that XDY-CS might ameliorate virus-induced endothelial dysfunction by modulating the PKC pathway (Fig. 7).

Discussion

Disruption of the pulmonary microvascular endothelial barrier can lead to the movement of fluid into the pulmonary air spaces, ultimately resulting in ARDS, acute lung injury, or pulmonary edema.[18,19] Microfilaments (such as actin filaments) are closely linked with vascular endothelial permeability. F-actin rearrangement leads to stress fiber formation, the stretching of which in turn contributes to paracellular gap formation and eventually to permeability increases.[20]

ERM-family proteins are crucial in regulating cell structures and functions. They serve as linkers between the plasma membrane and the actin cytoskeleton via N-terminal binding to membrane-adhesion molecules and C-terminal binding to actin. A conserved threonine residue is found in their respective C-terminal regions, namely T567 in ezrin, T564 in radixin, and T558 in moesin. An important mechanism of ERM-family regulation occurs through phosphorylation of their respective conserved threonine residues.[21] Phosphorylation of the conserved threonine residue causes conformational changes in ERM, which unmasks binding sites for effector proteins.[22] Rho kinase, p38 MAPK, and PKC are 3 kinases that are thought to phosphorylate ERM proteins. Previous studies have also provided evidence that these kinases modulate endothelial cell permeability.[21,22]

Various stimuli can promote ERM phosphorylation in endothelial cells. The p-ERM protein mainly localizes to the border of PMVECs, where it can link cytoskeletal and membrane elements, leading to the formation of stress fibers and paracellular gaps, eventually contributing to permeability increases. Previously, it was reported that ERM phosphorylation induced by TNF-α may trigger permeability increases in human PMVECs via the p38 MAPK and PKC pathways.[20] Previous findings also showed that thrombin[23] and 2-methoxyestradiol[24] can mediate endothelial permeability increases by ERM phosphorylation via the PKC pathway. ERM protein phosphorylation via the p38 MAPK and Rho/ROCK pathways can also participate in modulating endothelial permeability induced by advanced glycation end products.[25] Previously, we showed that IV infection increased microvascular leakage in PMVECs, with the primary mechanism being related to activation of the Rho/ROCK, p38 MAPK, and PKC pathways, ultimately leading to ERM phosphorylation.[11]

XDY is a classic traditional medicine that is used for treating viral pneumonia induced by IV infection. Previously, we showed that XDY administration reduced mortality rates in mice with viral pneumonia.[10] Results from this prior study demonstrated that XDY reduced virus-induced permeability increases, as well as pulmonary inflammation and vascular injuries induced by IV. In addition, it was confirmed that a dosage of 13.8 g/kg (equivalent to the clinical dosage) was the most effective.
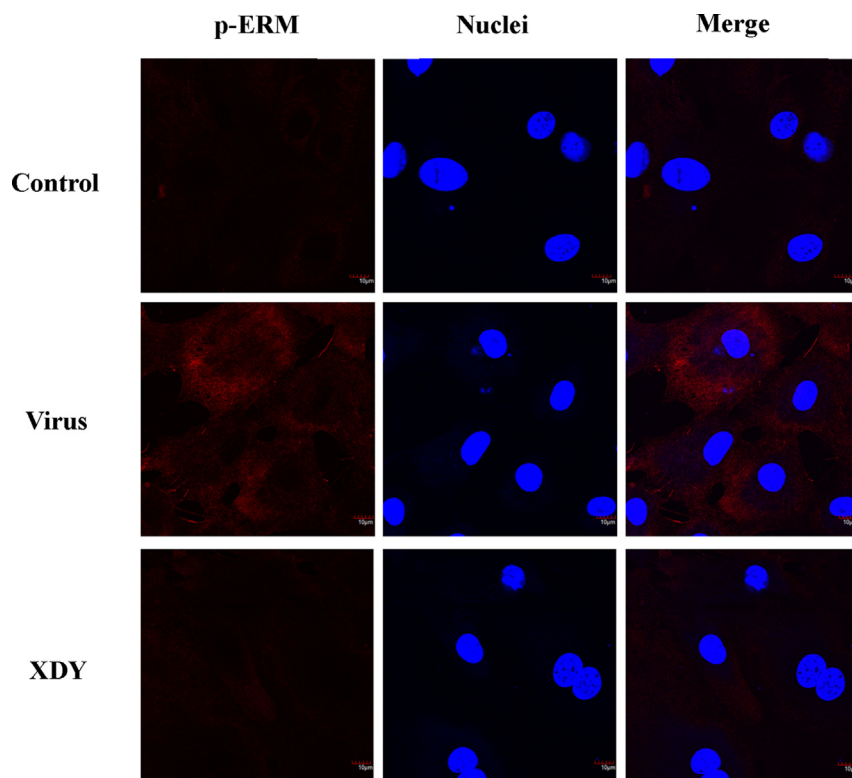
Fig. 4 Effect of XDY-CS on p-ERM distribution in IV-infected PMVECs (×60).Scale bars, 10 μm. After PMVECs were treated as indicated for 24 h, the distribution of p-ERM (red) and nuclei (blue) were examined by confocal microscopy. Representative data from 3 independent experiments are shown. Three replicates were performed in each experiment.
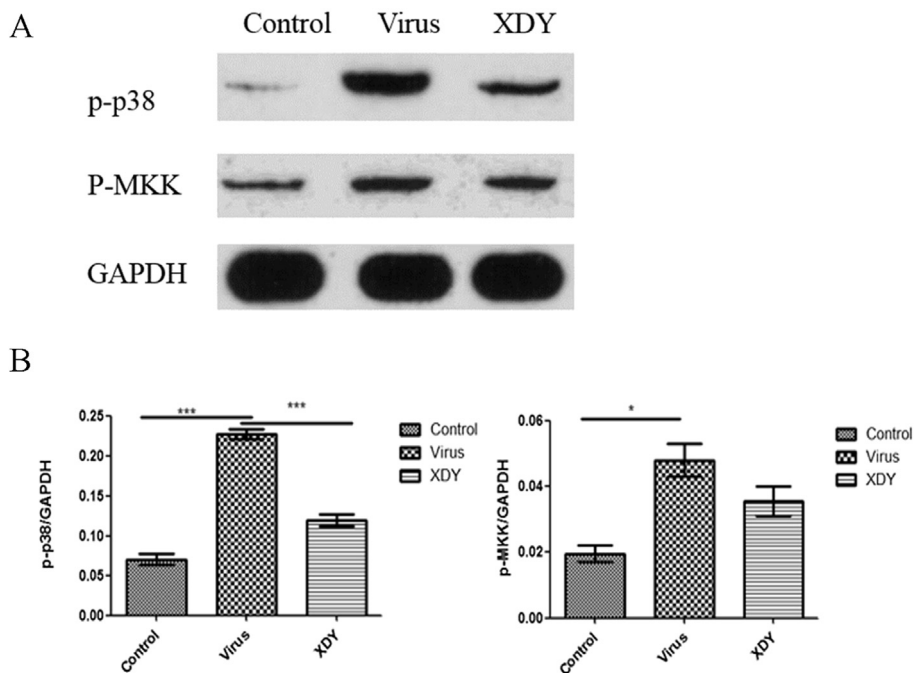

Fig. 5 Effect of XDY-CS on p-MKK and p-p38 levels in IV-infected PMVECs. (A) The production of p-p38 and p-MKK was analyzed by western blotting. GADPH was detected as an internal reference. (B) Quantitative evaluation of p-MKK and p-p38 bands by densitometry. Three independent experiments were performed in three replicates. The data shown are expressed as the mean (SEM). *: $P < .05$; ***: $P < .001$.
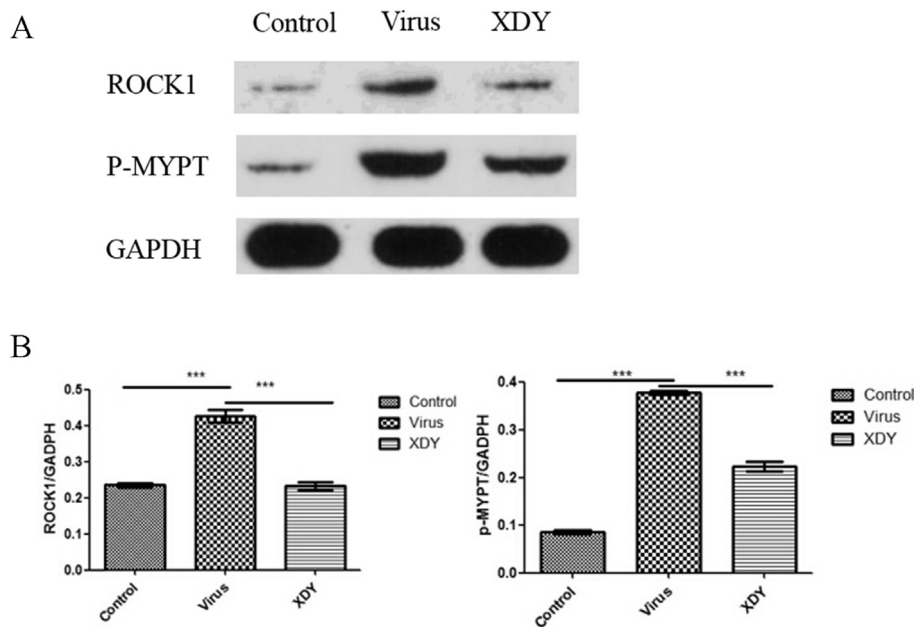
Fig. 6 Effect of XDY-CS on ROCK1 and p-MYPT production in IV-infected PMVECs. (A) ROCK1 and p-MYPT levels were analyzed by western blotting. GADPH was detected as an internal reference. (B) Quantitative evaluation of ROCK1 and p-MYPT bands by densitometry. Three independent experiments were performed in three replicates. Data are expressed as the mean (SEM). ***: $P < .001$.

Therefore, to gain insight into the mechanism whereby XDY protects the vascular endothelium, we studied the effects of XDY-SC in mice at a clinical-dose equivalent on F-actin and ERM-related pathways in IV-infected PMVECs.
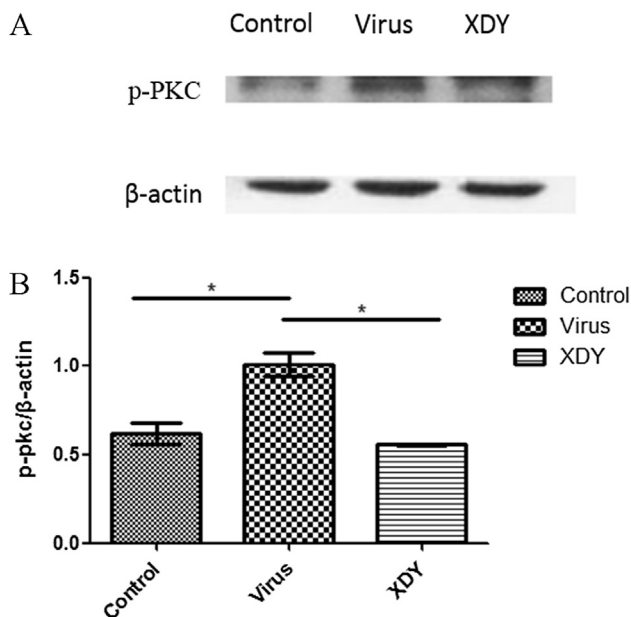

Fig. 7 Effect of XDY-CS on p-PKC production in IV-infected PMVECs. (A) The production of p-PKC was analyzed by western blotting. β-actin was detected as an internal reference. (B) Quantitative evaluation of p-PKC bands by densitometry. Three independent experiments were performed in three replicates. Data are expressed as the mean (SEM). *: $P < .05$.

In the study, XDY-CS dramatically reduced IV-induced stress fiber formation and F-actin accumulation in the cytoplasm. However, the difference of F-actin expression between virus group and XDY group was not statistically significant, suggesting that XDY-CS mainly alleviated F-actin rearrangement rather than reducing its expression.

We also determined the effect of XDY-CS on phosphorylation of the ROCK substrate MYPT. Previous data demonstrated that ROCK is upregulated in endothelial cells infected with virus.[26] The activation of ROCK promotes MYPT phosphorylation, thus activating MLC and promoting actin-filament polymerization. That MYPT expression was reduced in XDY-CS-treated PMVECs indicated that IV-induced F-actin reorganization was reversed by XDY-CS via the inhibition of MLC phosphorylation. The integrity of endothelial cell cytoskeletons, which are mediated by MLC phosphorylation, is indispensable for endothelial cell functions. MYPT phosphorylation can promote ERM phosphorylation, suggesting that common pathways may be shared between MLC and ERM.[27] Therefore, the effect of XDY-CS on F-actin reorganization might be linked with MLC regulation, a possibility that we intend to study in the future.

Interestingly, the cytoskeletal changes observed were not solely linked with the hyperpermeability of PMVECs, but were also related to virus replication. Actin polymerization is augmented in IV-infected cells, which is accompanied by activation of the Raf/MEK/ERK and PKC pathways, as well as calcium and phospholipase C production.[28–30] F-actin rearrangement can facilitate viral transportation into the nucleus via gene regulation or activation of the F-actin transportation system in the cytoplasm.[26] Although we did not observe that XDY inhibited viral replication in IV-infected PMVECs (data not shown), which might have

been due to the interference of serum with virus replication in vitro, we did detect the reduction of viral titers in lung tissue of IV-infected mice. Because F-actin rearrangement is involved in IV replication, the ability of XDY to inhibit IV replication in vivo might be due to its capacity to reverse IV-induced F-actin reorganization. However, whether XDY inhibits IV replication by interfering with ERM phosphorylation remains unclear, since the role of ERM phosphorylation in IV replication remains uncertain, which merits further investigation.

Competing interests

The authors have declared that no competing interests exist.

Acknowledgments

References

1. Michael P, Brabant D, Bleiblo F, et al. Influenza A induced cellular signal transduction pathways. *J Thorac Dis*. 2013;5: S132—S141.
2. Dushianthan A, Grocott MP, Postle AD, Cusack R. Acute respiratory distress syndrome and acute lung injury. *Postgrad Med J*. 2011;87:612—622.
3. Armstrong SM, Mubareka S, Lee WL. The lung microvascular endotheliumas a therapeutic target in severe influenza. *Antivir Res*. 2013;99:113—118.
4. Short KR, Kroeze EJ, Fouchier RA, Kuiken T. Pathogenesis of influenza-induced acute respiratory distress syndrome. *Lancet Infect Dis*. 2014;14:57—69.
5. South East Asia Infectious Disease Clinical Research Network. Effect of double dose oseltamivir on clinical and virological outcomes in children and adults admitted to hospital with severe influenza: double blind randomised controlled trial. *BMJ (Clin Res ed.)*. 2013;346:f3039.
6. Wu JT. *Wen Bing Tiao Bian*. Beijing, China: People's Medical Publishing House; 2005 [Chinese].
7. Wang Y, Zuo H, Li FR, et al. Clinical efficacy observation of Yinqiaosan for H1N1 influenza. *J Sichuan Tradit Chin Med*. 2010;28:73—74 [Chinese].
8. Zhang ZY, Zhang JG, Zhang JM, Wang ZS. Perceptions of SARS, termed lunar epidemic febrile disease in the work of Wenbing Tiaobian. *Hebei J TCM*. 2003;25:565—566 [Chinese].
9. Li CX. Modified *Xijiao* dihuang decoction's effects in treating viral pneumonia. *Heilongjiang J Tradit Chin Med*. 2001;6:42 [Chinese].
10. Hao Y, Li JQ, Wu Y, Wu J, Lu GL, Huang QF. Influences of *Xijiao*dihuang Decoction combined with Yingqiao Power on virus titer and pathological changes of lung tissue in mice with influenza viral pneumonia. *J Beijing Univ Chin Med*. 2010;33: 739—744 [Chinese].
11. Zhang CY, Wu Y, Xuan ZN, et al. p38MAPK, Rho/ROCK and PKC pathways are involved in influenza-induced cytoskeletal rearrangement and hyperpermeability in PMVEC via phosphorylating ERM. *Virus Res*. 2014;192:6—15.
12. Haas MA, Vickers JC, Dickson TC. Rho kinase activates ezrin-radixin-moesin (ERM) proteins and mediates their function in cortical neuron growth, morphology and motility in vitro. *J Neurosci Res*. 2007;85:34—46.
13. Hébert M, Potin S, Sebbagh M, Bertoglio J, Bréard J, Hamelin J. Rho-ROCK-dependent ezrin-radixin-moesin phosphorylation regulates Fas-mediated apoptosis in Jurkat cells. *J Immunol*. 2008;181:5963—5973.
14. Ng T, Parsons M, Hughes WE, et al. Ezrin is a down-stream effector of trafficking PKC-integrin complexes involved in the control of cell motility. *EMBO J*. 2001;20:2723—2741.
15. World Health Organization. Principles of laboratory animal care. *World Health Organ Chron*. 1985;39:51—56.
16. Jiang X, He Z, Liu Y. The pharmachemical research on the blood serum of Yinqiaosan. *J Hubei College TCM*. 2007;9:15—16 [Chinese].
17. Zhang H, Sun GY. LPS induces permeability injury in lung microvascular endothelium via AT (1) receptor. *Arch Biochem Biophys*. 2005;441:75—83.
18. Maniatis NA, Orfanos SE. The endothelium in acute lung injury/acute respiratory distress syndrome. *Curr Opin Crit Care*. 2008;14:22—30.
19. Teijaro JR, Walsh KB, Cahalan S, et al. Endothelial cells are central orchestrators of cytokine amplification during IV infection. *Cell*. 2011;146:980—991.
20. Mong PY, Petrulio C, Kaufman HL, Wang Q. Activation of Rho kinase by TNF-alpha is required for JNK activation in human pulmonary microvascular endothelial cells. *J Immunol*. 2008; 180:550—558.
21. Koss M, Pfeiffer 2nd GR, Wang Y, et al. Earin/radixin/moesin proteins are phosphorylated by TNF-α and modulate permeability increases in human pulmonary microvascular endothelial cells. *J Immunol*. 2006;176:1218—1227.
22. Smith WJ, Nassar N, Bretscher A, Cerione RA, Karplus PA. Structure of the active N-terminal domain of Ezrin. Conformational and mobility changes identify keystone interactions. *J Biol Chem*. 2003;278:4949—4956.
23. Adyshev DM, Dudek SM, Moldobaeva N, et al. Ezrin/radixin/moesin proteins differentially regulate endothelial hyperpermeability after thrombin. *Am J Physiol Lung Cell Mol Physiol*. 2013;305:L240—L255.
24. Bogatcheva NV, Zemskova MA, Gorshkov BA, et al. Ezrin, radixin, and moesin are phosphorylated in response to 2-methoxyestradiol and modulate endothelial hyperpermeability. *Am J Respir Cell Mol Biol*. 2011;45:1185—1194.
25. Guo X, Wang L, Chen B, et al. ERM protein moesin is phosphorylated by advanced glycation end products and modulates endothelial permeability. *Am J Physiol Heart Circ Physiol*. 2009;297:H238—H246.
26. Haidari M, Zhang W, Ganjehei L, Ali M, Chen Z. Inhibition of MLC phosphorylation restricts replication of IV—a mechanism of action for anti-influenza agents. *PLoS One*. 2011;6:e21444.
27. Canals D, Roddy P, Hannun YA. Protein phosphatase 1α mediates ceramide-induced ERM protein dephosphorylation: a novel mechanism independent of phosphatidylinositol 4,5-biphosphate (PIP2) and myosin/ERM phosphatase. *J Biol Chem*. 2012; 287:10145—10155.
28. Arora DJ, Gasse N. IV hemagglutinin stimulates the protein kinase C activity of human polymorphonuclear leucocytes. *Arch Virol*. 1998;143:2029—2037.
29. Zhu L, Ly H, Liang Y. PLC-γ1 signaling plays a subtype-specific role in postbinding cell entry of influenza A virus. *J Virol*. 2014; 88:417—424.
30. Pleschka S, Wolff T, Ehrhardt C, et al. IV propagation is impaired by inhibition of the Raf/MEK/ERK signalling cascade. *Nat Cell Biol*. 2001;3:301—305.